# Temporal evolution of cell focal adhesions: experimental observations and shear stress profiles

**D. Raz-Ben Aroush,[a] R. Zaidel-Bar,[b] A. D. Bershadsky[b] and H. D. Wagner*[a]**

***Received 18th March 2008, Accepted 31st July 2008***
***First published as an Advance Article on the web 10th September 2008***
**DOI: 10.1039/b804643n**

Live cells create adhering contacts with substrates *via* focal adhesion (FA) sites associated with the termini of actin stress fibers. These FA 'anchors' enable cells to adhere firmly and locally to a substrate, and to generate traction that enables cell body displacement. Using time-lapse video microscopy, we have monitored the spontaneous anisotropic changes in FA size and shape, resulting from molecular reorganization of the adhesion sites in live, non-motile rat embryonic fibroblasts adhering to fibronectin-coated glass surfaces. The resulting experimental data on FA growth, saturation and decay is compared with predictions from a number of biophysical models. We find that the growth and saturation regimes for all FAs exhibit a consistent, recurring pattern, whereas the disassembly regime exhibits erratic behavior. We observe that the maximum size of FA areas depends on the FA growth rate: larger FA areas are formed as the growth rate increases. Using a composite mechanics model by which the evolution of the shear stress profile along the FA region can be calculated, we suggest that FA saturation is triggered either by the reaching of a minimum shear stress threshold at the FA back edge, or of a maximum difference between the maximum and minimum shear stress along the FA site.

## Introduction

In many cell types, adhesion to an extra-cellular matrix (ECM) plays a significant role in cellular processes such as cell growth, differentiation, mobility, apoptosis and tissue formation. ECM adhesions can be classified by molecular and structural criteria into 'focal contacts', located mainly at the cell periphery, and 'fibrillar adhesions' which are elongated or beaded structures located more centrally in cells.[1–5] 'Focal contacts' are often sub-divided into 'dot-like' contacts on the one hand, which are adhesion sites of about one square micron termed focal complexes (or FXs), and more elongated structures up to 10 μm in length on the other hand, known as focal adhesions (FAs). FAs serve as 'anchors' that permit a cell to adhere with regulated strength to a substrate, and to generate traction that enables cell migration. FAs are complex multi-molecular assemblies linked on one side to the ECM *via* trans-membrane receptors, and on the other side to the termini of actin stress fibers within the cytoskeleton. Tension along these actin fibers is generated by myosin motors and is tightly regulated by the cell. FAs react to mechanical signals[6–8] by producing an array of biochemical processes which, in turn, can generate structural and mechanical changes in the cells consecutively leading to additional mechanical and biochemical effects.

It has been demonstrated that cell–ECM adhesions can sense and respond to the ECM rigidity[9] as well as the spatial organization of the extra-cellular environment at the nanometre scale.[10] When a force is applied to the FAs—whether the force is external to the cell (from shear flow, or from the action of a pipette for example) or internally applied by the cell itself through stress fibers—FAs react by increasing their length and width, thus increasing their area. This increase is anisotropic as it always occurs in the direction of the internal force applied by the stress fibers (roughly toward the cell nucleus), defined as the front edge of the FA.[11] The opposite edge of the FA is called the back (or rear) edge (Fig. 1). Fair evidence of a correlation between the applied tangential force and the orientation and contact area of FAs has recently been found,[6,12,13] leading to an approximate stress of 5.5 kPa (or nN $\mu m^{-2}$). Although not stated explicitly, from a physical viewpoint this is the average FA–ECM adhesive shear stress: formally it has the technical inconsistency of not

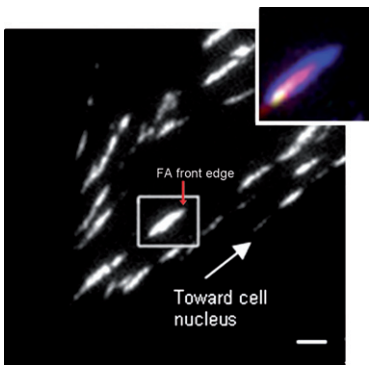


**Fig. 1** FA evolution at three successive times ($t_1<t_2<t_3$). The FA is shown in the square (main picture) at time $t_3$. The insert is a superposition of the growing FA area at times $t_1$, $t_2$ and $t_3$, and is colored in green, red and blue at times $t_1$, $t_2$ and $t_3$, respectively. The resultant white color is the superposition of all colors, whereas the purple color results from the combination of red ($t_2$) and blue ($t_3$). The front edge of the FA is indicated by the red arrow. The white arrow points in the direction of the cell nucleus. Scale bar: 2 μm.

[a]*Department of Materials and Interfaces, Weizmann Institute of Science, Rehovot 76100, Israel. E-mail: Daniel.wagner@weizmann.ac.il*
[b]*Department of Molecular Cell Biology, Weizmann Institute of Science, Rehovot 76100, Israel*

 

dropping to a nil value at zero FA area, and of providing a mean value rather than a full profile of stress along the FA region which would lead to further understanding of localized adhesion mechanisms. Such a stress profile was recently proposed.[14]

Although this area of biophysics is currently the subject of extensive experimental[13,15–18] and theoretical[14,19–24] research, the mechano-sensing process is not fully understood. One important facet of this intricate dynamic biochemical–mechanical coupling is the ability of a cell to transfer (and receive) mechanical signals—stress or strain—*via* the actin bundles to (and from) an ECM. Recently we suggested a theoretical model[14] in which cell–ECM adhesion was investigated using a shear-lag type mechanical model classically used in composite material science. The entire shear stress profile along the interface between a single 'static' FA (at a 'frozen' moment during the FA growth process) and the ECM could be calculated as a function of various material and geometrical characteristics of the adhesion region. It was found that the interfacial shear stress reaches a maximum value at the front edge of the FA site. The shape of the shear stress profile along the cell–ECM interface suggests a likely triggering mechanism for the biochemical feedback activity responsible for the temporal change (growth or decay) of the adhesion region. Similarly, Nicolas *et al.*[19] hypothesized that force-induced deformations trigger the biochemical response of FAs.

The present paper addresses the issue of the spontaneous (in the absence of any force or perturbation applied from outside the cell) anisotropic increase/decrease in length and width of FAs. The dynamics of the single FA growth/shrinkage process is examined quantitatively through microscopic inspection of live, quasi-stationary fibroblast cells adhering to fibronectin-coated glass surfaces, and an interpretation of the data is provided by means of a composite model[14] for the shear stress profile along the FA.

## Experimental

### Cell culture

A cell line of rat embryo fibroblasts (REF 52) stably expressing paxillin yellow fluorescence protein (YFP)[25] were plated on a rigid (glass) substrate coated with fibronectin (5 μg $ml^{-1}$, 1 h, 37 °C) and incubated for 24 h at 37 °C in Dulbecco's Modified Eagle's Medium (DMEM) with 10% fetal calf serum (FCS) and antibiotics. During the experiment the cells were maintained in DMEM containing 25 mM HEPES, without Phenol Red and riboflavin (Biological Industries) and supplemented with 10% FCS, which was used in order to maintain a pH of 7.04 throughout the experiments. REF 52 cells are mostly populated by large, mature and stable FAs. Paxillin is a well established adapter component of FA and is a good marker for studying adhesion evolution, including assembly, stabilization and disassembly.[26–28]

### Dynamic measurement of FA area

Time-lapse movies were recorded using the Real Time (RT) DeltaVision System (Applied Precision Inc., Issaquah, WA, USA), consisting of an Olympus IX71 inverted microscope equipped with a CoolSnap HQ camera (Photometrics, Tucson, AZ, USA) and a weather station temperature controller, operated by SoftWoRx and Resolve3D software (Applied Precision Inc.). Images (see Fig. 1) were acquired with an Olympus planApoN 60X/1.42 objective, with or without an additional 1.6× auxiliary magnification. The evolution of individual FAs was monitored for an hour and a half with either 2.5 or 3 min time intervals between images. Twenty stabilized, mature FAs located at the cell periphery (similar to the FA shown in Fig. 1) were selected for analysis. As far as we can tell, this set included all mature FAs. A total of approximately 600 images were thus collected. Image analysis was carried out using Priism software for Linux (http://www.msg.ucsf.edu/IVE/Download). Assuming that the FA is rectangular in shape, the temporal evolution of a number of FA geometrical characteristics, including the length ($L_{FA}$), width ($d_{FA}$), and area ($A_{FA}$), was monitored and subsequently correlated with the adhesion strength profile developed in our previous work.[14]

### Generation of 3D images

Since the signal remained consistently below saturation levels, the fluorescent signal may be linearly correlated to the concentration of paxillin at the FA site. Color-coded 3D images, such as those presented in Fig. 2, were generated using MatLab to demonstrate the augmentation and reduction in light intensity which accompanies protein density and thus FA growth and decay, as observed from the time-lapse movies.

## Results and discussion

The adhesion dynamics of single FA sites was monitored in detail to characterize FA growth and decay induced purely by the cell contractility (no external perturbation). This led us to examine the relationship between the experimentally observed FA evolution and the associated shear stress profile generated at the FA–ECM interface, and to compare these experimental data with various recent theoretical schemes. The following specific questions were addressed: (i) do FA sites grow (and then decay) according to a well-defined recurrent geometric pattern, or is there a significant element of randomness in the time evolution of FA growing/decaying sites? (ii) How are temporal changes in FA geometry reflected in the associated interfacial shear stress profile? (iii) What are the quantitative implications on the model of the observed geometrical evolution of FAs? (iv) Can the experimental data presented here help in the selection of a 'best-fit' theoretical scheme for FA growth and decay?

Our observations of the temporal evolution of single FAs in REF 52 cells reveal three sequential regimes: FA growth, saturation, and disintegration, with distinct trends, as now described and discussed quantitatively. We refer to Fig. 3, in which the growth (3a, 3b) and saturation (3c, 3d) regimes of two FAs are clearly observed. The cell nucleus (not shown) is located towards the upper side of the images; therefore on those pictures the back (or rear) edge of the FA is at the bottom of the FA and the front edge at its top, respectively.

### (i) Regime I—FA growth

Fig. 2a, 3a and 3b show that, whereas the back edge of the FA remains stationary, the front edge is growing significantly with

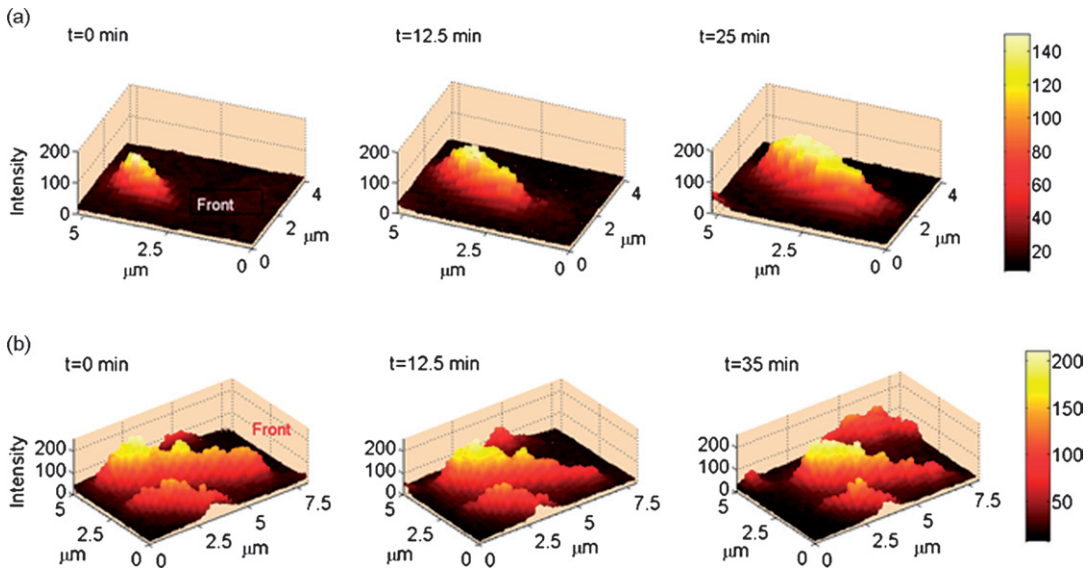


**Fig. 2** Color-coded 3D images demonstrating change in protein density with time for (a) a growing FA and (b) a disintegrating FA.

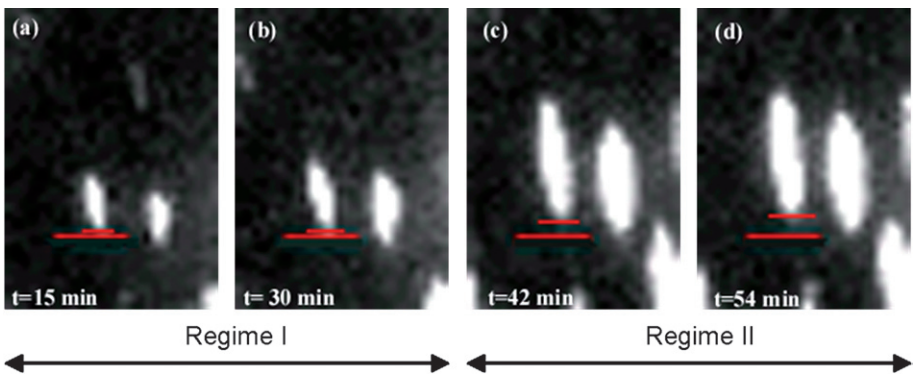


**Fig. 3** FA evolution at four successive times in regimes I and II. The lower red line is drawn at the same position for all four images while the upper red line is positioned at the back edge of the FA site. The gap increase between the two lines indicates movement of the FA back edge toward the cell nucleus.

time: such inhomogeneous and anisotropic FA expansion has often been observed in growing FAs. It most certainly implies that, in regime I at least, most FA sites grow by protein assembly at the front edge only, rather than by a positive difference between FA protein assembly and disassembly rates as recently suggested by Besser and Safran.[23] It may also be that the FA site grows in this manner as a result of a two step process in which the FA proteins are pushed toward the front edge due to protein accumulation at the back edge. Our recent composite mechanics model[14] predicts that the FA–ECM interfacial shear stress reaches a minimum value, $\tau_{min}$, at the back edge of the FA and a maximum value, $\tau_{max}$, at the front edge (Fig. 4), it can be inferred that the highly stressed front edge, where maximum deformations occur, is likely to be the zone where biochemical signals are preferentially triggered by the cell and new proteins are being recruited,[22] inducing directional growth of the adhesion site[12] as observed. The different mechanisms suggested here for the observed growth at the front edge can be experimentally determined by a bleaching experiment (such as described in ref. 23).

### (ii) Regime II—FA area saturation

Fig. 3c and 3d reveal that beyond a certain point in time, FAs do not grow any further and a saturation state is reached where, as seen, an apparent treadmill-like action, generated by protein disassembly at the FA back edge and protein assembly at the front edge (elsewhere often confusingly termed 'sliding'[19] or 'crawling'[22]) is generally assumed to take place. The saturation state is preserved for some time, without overall FA disintegration. Since we have assumed that a strong correlation exists between protein concentration at the FA site (as reflected by the intensity of paxillin fluorescence) and FA–ECM adhesion strength, the observed constant protein concentration in regime II presumably means that the interface strength remains constant, which translates into a treadmill-like translation of the

 

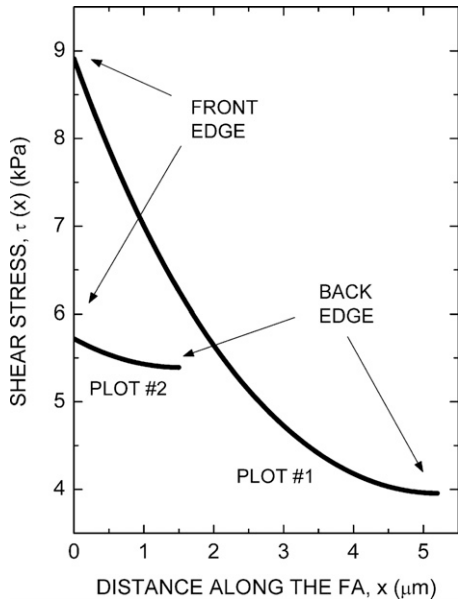


**Fig. 4** Typical calculated shear stress profiles along the length of a long (plot #1) and short (plot #2) FA.

FA rather than 'sliding'. This kind of treadmill-like action has been proposed previously[29] and recently verified in migrating cells.[30]

### (iii) Regime III—FA disintegration

Beyond a certain time limit, disintegration of the FA occurs. The disintegrating pattern is gradual and appears at random spots along the FA (see example in Fig. 2b), and is accompanied by significant protein intensity changes, reflecting the erratic disassembly rate along the FA. The disintegration process occurred in about 80 min, much longer than the growth process.

Fig. 5 shows the area increase for 12 single FAs as a function of time, up to the saturation limit. The disintegrating process was subsequently observed using 8 additional single FA sites but an evolution plot such as Fig. 5 cannot be made since FA disintegration was found to be erratic. The main observations are as follows: (i) initial FA growth is linear in time; (ii) saturation is consistently reached after 35 to 45 min; (iii) FAs can grow at various rates (Fig. 5), but all of them cease to grow at approximately equal times [as stated in (ii)], with the consequence that smaller FAs are unable to reach the large areas achieved by fast-growing FAs. This is further discussed later.

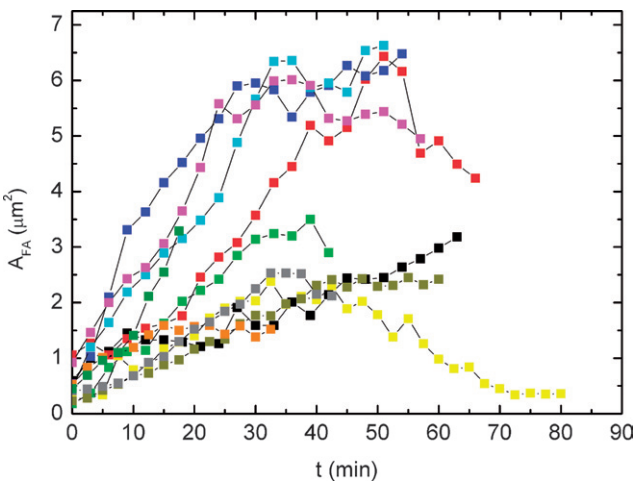


**Fig. 5** Temporal evolution of FA area for 12 different FA sites.

The FA area *vs.* time plot presented in Fig. 6a (which is a typical example) is a composite of separate measurements of the length and width of FAs (Fig. 6b and 6c). No decay could be observed for this specific FA. All three parameters, $L_{FA}$, $d_{FA}$ and $A_{FA}$ increase linearly with time in regime I, from $t = 0$ to $t \approx 40$ min. When data from all specimens are included $L_{FA}$ increases by an average factor of 4.19, with a standard deviation (SD) = 1.25, $d_{FA}$ increases by an average factor of 1.91 (SD = 0.46) and $A_{FA}$ increases by an average factor of 8.39 (SD = 3.81) from its initial size. Thus, in regime I all three geometric parameters are observed to increase, albeit at different rates, leading to the familiar anisotropic FA growth. In regime II, however, $L_{FA}$ is seen to grow at a much milder rate than in regime I (by an average growth factor of 1.07, SD = 0.051, from its initial size when data from all specimens are included), and $d_{FA}$ is seen to slightly decrease (by an average factor of 0.95, SD = 0.025, from its initial size when all specimens are included). Combining the length increase with the slight width decrease results in the observed FA area saturation. We emphasize that (i) at the saturation limit (regime II) the protein assembly rate at the front edge is still slightly larger than the disassembly rate at the back edge, and the measured constancy of the FA area results from the compensating lateral shrinkage of the FA; (ii) in rare cases the lengthwise treadmill action was not observed and the FA length kept on growing from the front edge (in other words, there was only protein assembly without disassembly).

This growth and saturation pattern, leading to anisotropic growth features, was observed for all the FAs under consideration. A major question of interest, discussed below, concerns the nature of the triggering of the FA area saturation onset.

The effect of the changing FA geometry during the various stages of maturation on the FA–ECM interfacial shear stress profile may be examined using a composite mechanics model.[14] The shear stress profile at the FA–ECM interface is given by:

$$\tau(x) = 0.125\sigma_{actin}\pi d_{FA}\alpha[coth(\alpha L_{FA})cosh(\alpha x) - sinh(\alpha x)] \quad (1)$$

where $L_{FA}$ is the FA length, $d_{FA}$ is the FA width, $\sigma_{actin} = F_{actin}/A_{actin}$, where $A_{actin}$ is the actin fiber cross-section (assumed to be equal to the FA cross-section) and $F_{actin}$ is the variable force generated by the myosin motors connected to the actin stress fiber. This force was not measured here[31] thus we have used the approximation[6] $F_{actin} = 5.5A_{FA}$. The parameter $\alpha$ includes material and geometric parameters which control the mechanical behavior and interactions at the cell–ECM interface. As described elsewhere,[14] we use Nayfeh's expression:

$$\alpha^2 = \frac{2}{r_{actin}{}^2 E_{actin} E_{ECM}} \left[\frac{E_{actin}V_{actin} + E_{ECM}V_{ECM}}{\frac{V_{ECM}}{4G_{actin}} + \frac{1}{2G_{ECM}}\left(\frac{1}{V_{ECM}}\ln\frac{1}{V_{actin}} - 1 - \frac{V_{ECM}}{2}\right)}\right] \quad (2)$$

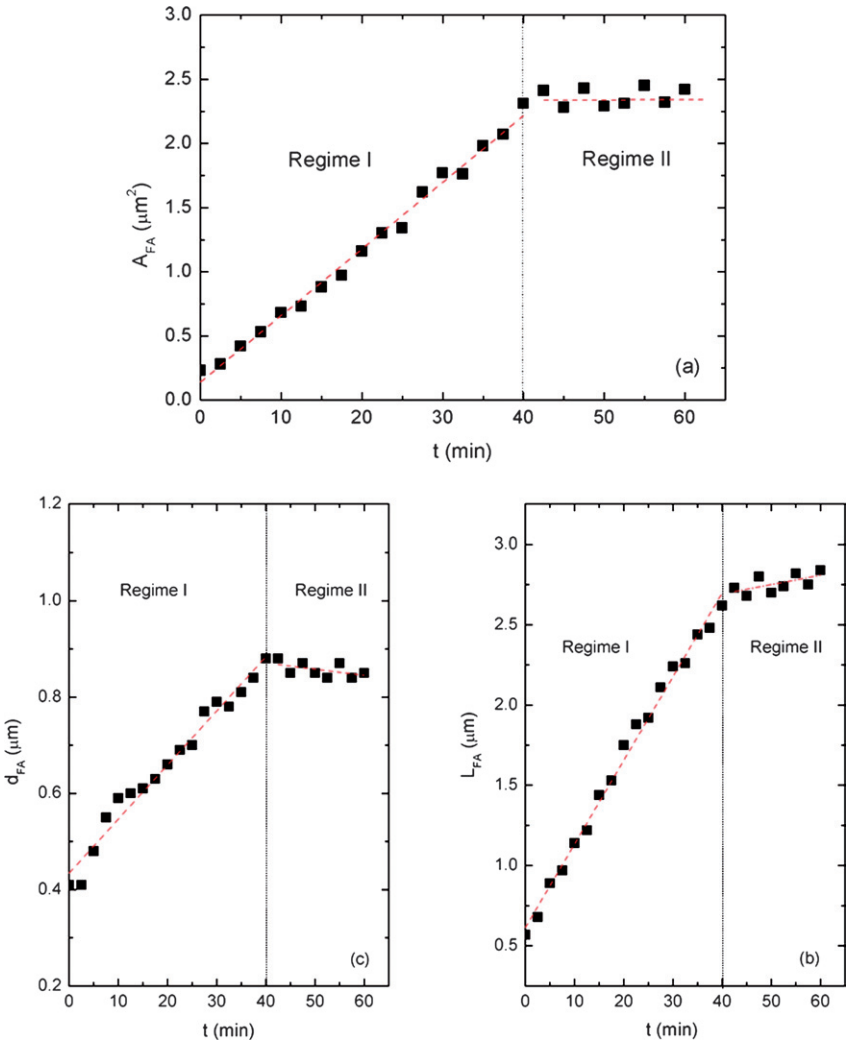


**Fig. 6** Typical plots constructed from dynamic image analysis raw data for a single FA site, including (a) FA area ($A_{FA}$), (b) FA length ($L_{FA}$) and (c) FA width ($d_{FA}$) evolution with time.

where $E$, $G$ and $V$ denote the Young's modulus, shear modulus and volume fraction, respectively. The basic features of the shear stress profile given in eqn 1 include (i) a maximum value at $x = 0$ and a minimum at $x = L_{FA}$; (ii) a monotonic, non-linear decrease along the length, from $x = 0$ to $x = L_{FA}$. The temporal change in the shear stress profile (eqn 1) during the growth of a single FA site results only from the experimentally measured evolving geometry of the FA, as the selected values for the material parameters ($E_{ECM} = 20$ kPa, $E_{actin} = 2$ GPa, $\nu_{ECM} = 0.35$ and $\nu_{actin} = 0.3$) are assumed to remain constant. This establishes a correlation between the mechano-sensing feature, expressed through the composite mechanics model, and the observed temporal changes of the FA geometry.

As an example, Fig. 7 shows the calculated shear stress profile using five successive snapshot views of the growth of a single FA. The shear stress is maximum at the front edge [$\tau(x = 0)$] and minimum at the back edge [$\tau(x = L_{FA})$]. The shear gradient $\Delta\tau$=( $\tau_{max} - \tau_{min}$) increases with time, as $A_{FA}$ increases through regime I, and then stabilizes as $A_{FA}$ saturates in regime II. The temporal evolution of $\tau_{max}$ and $\tau_{min}$ is shown in Fig. 8. As seen, $\tau_{max}$ first increases almost linearly in regime I, then stabilizes in regime II. On the other hand, $\tau_{min}$ decreases (but more mildly) in regime I.

In terms of protein assembly/disassembly rates, in view of the shape of the stress profile along the FA, in regime I the rear edge of the FA are likely to be inactive (neither assembly nor disassembly) whereas the fast-growing front edge is actively recruiting new proteins. Whether the shear stress profile reflects protein activity or causes it is uncertain. In regime II where FA area saturation takes place, a treadmill-like behavior starts *via* protein assembly at the front and disassembly at the back. The observed continued mild increase in $L_{FA}$ means that the assembly rate at the front is slightly larger than the disassembly rate at the rear. What triggers this sudden change is an open question. The source may possibly be mechanical/physical if one assumes for example that molecular disassembly at the back edge is triggered when a specific critical value of $\tau_{min}$ (or $\Delta\tau$) is reached or overcome: $\tau_{min} < \tau_{min}^*$. In other words, as long as a threshold of $\tau_{min}^*$ (or $\Delta\tau^*$) is not reached the FA site will continue to grow (assemble) without disassembling at its rear edge. At the front

 

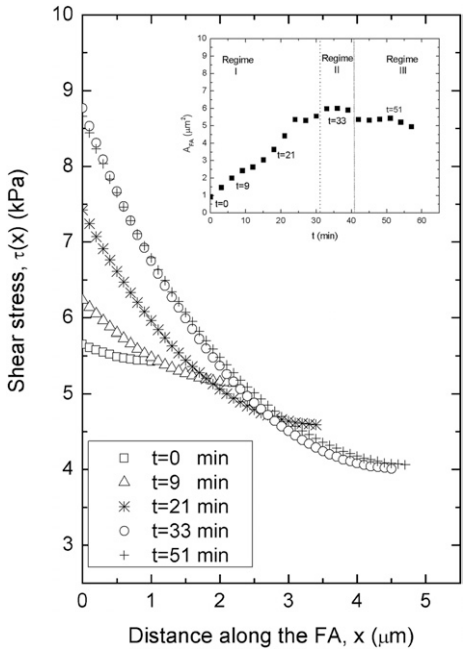


**Fig. 7** Evolution of shear stress profile during FA growth. Insert: corresponding evolution of FA area with time.

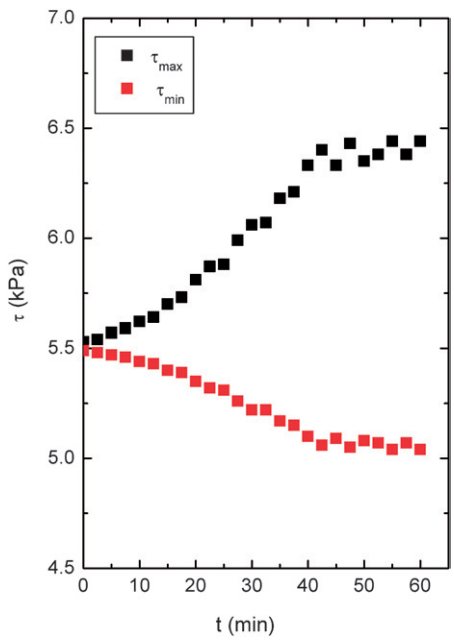


**Fig. 8** Variation in time of the maximum and minimum shear stress at the front and back edges of the FA site.

edge, as we have seen, protein assembly always proceeds, even at slow rates.

We also observe in Fig. 5 that FAs which grow fast (higher initial slopes) apparently also attain larger areas at saturation. This is indeed confirmed by the dependence seen in Fig. 9, where the maximum area reached by each FA is plotted against area growth rate. When the data is arbitrarily fitted by a sigmoid curve for clarity ($r^2 = 0.98$), a cut-off growth rate of 0.1 μm$^2$ min$^{-1}$ is apparent. A linear fit can also be used instead of a sigmoid but with a much lower regression coefficient ($r^2 = 0.79$). Such area *vs.* growth rate dependence is *a priori* not to be expected since slow-growing FAs could in principle continue to grow for longer times than fast-growing FAs, and eventually reach a similar total area. This is not observed. What is experimentally observed, however, is the appearance of a definite time cut-off, about 35–45 min from the start of the FA growth process, which determines the saturation area limit for all FAs, whether they grow fast or slow. Whether this cut-off is related to an absolute stress limit, or stress gradient limit, or simply a lifetime limit, is currently unclear. Equally uncertain is the biochemical trigger of the cut-off. We also observe that the larger saturation area limits are obtained when $\tau_{min}$ values are smaller, or alternatively with larger values of $\tau_{max}-\tau_{min}$ ($=\Delta\tau$). Although some studies were recently conducted to study the molecular composition and dynamics of cell–ECM adhesions,[27,29] little is known about how protein interactions are directly influenced by mechanical signals. Recently, by using different fluorescence fluctuation approaches, paxillin dynamics across single adhesions (nascent adhesions, growing adhesions, treadmilling adhesions and disassembling adhesions) was studied extensively.[30] However, studies which specifically correlate between mechanical stimuli and their biophysical/biochemical activity are still lacking. It is also uncertain why FA areas grow at varying rates, and what is the mechanism governing the rate of growth.

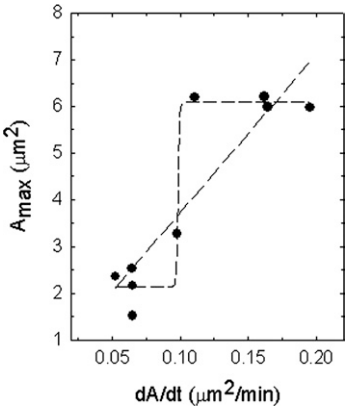


**Fig. 9** FA maximum area as a function of growth rate for 9 FA sites which reached a constant area size (regime II). The data is arbitrarily fitted by a straight line ($r^2 = 0.79$) and a sigmoid curve ($r^2 = 0.98$).

The decay regime (regime III) is random-looking, as can be seen from the erratic protein intensity patterns observed in this regime, see Fig. 2b. In this case the use of the composite model for the calculation of a decaying shear stress profile is impractical. Similarly, the identification of a mechanical triggering mechanism for FA disintegration using the composite mechanics model cannot be made. In order to better understand the disintegration mechanism, two experiments can be suggested: (i) the disintegration of single FA sites can be monitored in the presence of a drug that inhibits cell contractility which is known to induce FA disintegration by progressively eliminating the presence of the internally applied force. If indeed the decrease in force is the main factor that controls the disintegration process then the latter is not expected to be random. (ii) Actin stress fibers are

generally assumed to be connected to the FA site only in a direction parallel to the FA length. However, it may be that actin stress fibers connect also from various other directions, leading to the observed randomness of the disintegration process. Furthermore, it has been shown recently[25] that in mobile cells FA disintegrates due to specific microtubule-targeting interactions. This kind of mechanism may also play a role in the case of quasi-stationary cells. Predictions such as these could be tested by image analysis of fluorescence actin stress fibers and microtubules.

A number of scenarios,[16–24] all one-dimensional (only length changes are considered), have recently been proposed in the literature to explain FA dynamics. Shemesh *et al.*,[22] Besser and Safran,[23] and Nicolas and Safran[24] all predict FA growth and saturation, but base their arguments on different mechanisms, as discussed in ref. 23. Shemesh *et al.*[22] predict that FAs grow through progressive protein accumulation along the entire FA site, the driving force towards equilibrium being thermodynamic. Four regimes of self-assembly are predicted by Shemesh *et al.*,[22] but since the protein flux is calculated as a function of a number of force and anchoring parameters for a specific FA length, whereas in our experiments flux is time-dependent, a direct correlation between our experimental data and the model of Shemesh *et al.*[22] is problematic. Moreover, our observations clearly point to a pattern of FA growth at the front edge, likely reflecting protein accumulation restricted to the front edge of the FA, rather than all along its length. Moreover, it is evident from Fig. 2a that the profile of protein activity follows a non-linear trend, with the consequence that the corresponding stress profile itself is bound to be so (non-linear), as indeed is reflected in the composite mechanics model (eqn 1). All this seems to be at variance with the predictions of Shemesh *et al.*,[22] including the fact that a non-linear profile of protein activity (as experimentally observed here) is not expected to lead to a linear shear stress profile as in Shemesh *et al.*[22] Contrasting with the approach of Shemesh *et al*,[22] Nicolas and Safran[24] develop a model in which FA growth is triggered by mechano-sensing elements within the FA. However, the model in ref. 24 deals with FA growth on soft substrates, unlike those used here. Besser and Safran[23] extend the model of Nicolas to predict the dynamics of adsorption of cytoplasmatic proteins to the FA site on rigid surfaces. The velocities of both the front and back of the FA are predicted as a function of the increasing internally applied force. Under very small forces, FA sites are initially predicted to shrink, then to stabilize and finally to grow (Fig. 8 in ref. 23). We do not see this, probably because our experimental 'window' is confined to higher forces. Of Besser and Safran's three growth modes under relatively high forces (described in ref. 23 as RII, LIII, RIII), only one, LIII, in which FAs grow by protein assembling at the front edge and no protein accumulation at the back edge, was experimentally observed here (our regime I). Mode RII, in which FA growth is predicted because the assembly rate at the front is larger than the disassembly at the back (thus, a treadmill-like action), occurs according to Besser under lower forces. This is in contradiction with our (two-dimensional) experimental observations where a treadmill behavior occurs only later rather than earlier (regime II). As to Besser and Safran's mode RIII, where assembly (FA growth) is predicted at both the front and back edges, it is not experimentally observed here. Again, it must be emphasized that the models above (including our own composite model, which is restricted to the prediction of a shear stress profile, without growth mode) are one-dimensional whereas the experimental reality includes the length and width of FAs, thus a two-dimensional situation.

Finally, two or three fairly small neighboring (in a row) growing FA sites were occasionally observed to fuse, creating one large FA site. As far as we know, such fusion events are not reported in the literature or predicted by the different published models.

## Conclusions

In this experimental study of rat embryo fibroblasts we have monitored the geometrical dynamics of single FA sites using time-lapse microscopy. The growth and saturation regimes for all FAs exhibit a consistent, recurring pattern, whereas the disassembly regime exhibits an erratic behavior. We observed that the maximum size of the FA areas depends on the FA growth rate: larger FA areas are formed as the growth rate increases. Using a composite mechanics model by which the evolution of the shear stress profile along the FA region could be calculated, we suggest that the trigger for FA saturation is due to a threshold either of a minimum shear stress at the FA back edge or of a maximum difference between the maximum and minimum shear stress.

## Acknowledgements

The authors acknowledge stimulating interactions with, and comments from, Prof. Sam Safran, Prof. Benny Geiger and Prof. Nir Gov. This project was supported in part by the G.M.J. Schmidt Minerva Centre of Supramolecular Architectures, by the generosity of the Harold Perlman family and by the German-Israeli Foundation (GIF) for Scientific Research and Development. H.D. Wagner holds the Livio Norzi Professorial Chair in Materials Science.

## References

1 A. D. Bershadsky, I. S. Tint, Jr., A. A. Neyfakh and J. M. Vasiliev, *Exp. Cell Res.*, 1985, **158**, 433–444.
2 C. D. Nobes and A. Hall, *Cell*, 1995, **81**, 53–62.
3 B. Geiger and A. D. Bershadsky, *Curr. Opin. Cell Biol.*, 2001, **13**, 584–592.
4 E. Zamir and B. Z. Katz, *J. Cell Sci.*, 1999, **112**, 1655–1669.
5 E. Zamir, M. Katz, Y. Posen, N. Erez, K. M. Yamada, B. Z. Katz, S. Lin, D. C. Lin, A. D. Bershadsky, Z. Kam and B. Geiger, *Nat. Cell Biol.*, 2000, **2**, 191–196.
6 N. Q. Balaban, U. S. Schwartz, D. Rivelin, P. Goichberg, G. Tzur, I. Sabanay, D. Mahalu, S. A. Safran, A. D. Bershadsky, L. Adadi and B. Geiger, *Nat. Cell Biol.*, 2001, **3**, 466–472.
7 K. Burridge and M. Chrzanowska-Wodnicka, *Annu. Rev. Cell Dev. Biol.*, 1996, **12**, 463–519.
8 D. M. Helfman, E. T. Levy, C. Berthier, M. Shtutman, D. Riveline, I. Grosheva, A. Lachish-Zalait, M. Elbaum and A. D. Bershadsky, *Mol. Biol. Cell*, 1999, **10**, 3097–112.
9 R. J. Pelham and Y.-L. Wang, *Proc. Natl. Acad. Sci. U. S. A.*, 1997, **94**, 13661–13665.
10 E. A. Calvacanti-Adam, A. Micoulet, J. Blümmel, J. Auernheimer, H. Kessler and J. P. Spatz, *Eur. J. Cell Biol.*, 2006, **85**, 219–224.
11 R. Zaidel-Bar, Z. Kam and B. Geiger, *J. Cell Sci.*, 2005, **118**, 3997–4007.
12 D. Riveline, E. Zamir, N. Q. Balaban, U. S. Schwartz, T. Ishizaki, S. Narumiya, Z. Kam, B. Geiger and A. Bershadsky, *J. Cell Biol.*, 2001, **153**, 1175–1185.

 

13 J. L. Tan, J. Tien, D. M. Pirone, D. S. Gray, K. Bhadriraju and C. S. Chen, *Proc. Natl. Acad. Sci. U. S. A.*, 2003, **100**, 1484–1489.
14 D. Raz-Ben Aroush and H. D. Wagner, *Adv. Mater.*, 2006, **18**, 1537–1540.
15 P. M. Sheetz, D. P. Felsenfeld and C. G. Galbraith, *Trends Cell Biol.*, 1998, **8**, 51–54.
16 K. A. Beningo, M. Dembo, I. Kaverina, J. V. Small and Y. L. Wang, *J. Cell Biol.*, 2001, **153**, 881–888.
17 D. Choquet, D. P. Felsenfeld and M. P. Sheetz, *Cell*, 1997, **88**, 39–48.
18 K. J. Van Vliet, G. Bao and S. Suresh, *Acta Mater.*, 2003, **51**, 5881–5905.
19 A. Nicolas, B. Geiger and S. A. Safran, *Proc. Natl. Acad. Sci. U. S. A.*, 2004, **101**, 12520–12525.
20 I. B. Bischofs, S. A. Safran and U. S. Schwarz, *Phys. Rev. E*, 2004, **69**, 021911–021917.
21 U. S. Schwarz and S. A. Safran, *Phys. Rev. Lett.*, 2002, **88**, 0481021–0481024.
22 T. Shemesh, B. Geiger, A. D. Bershadsky and M. M. Kozlov, *Proc. Natl. Acad. Sci. U. S. A.*, 2005, **102**, 1283–12388.
23 A. Besser and S. A. Safran, *Biophys. J.*, 2006, **90**, 3469–3483.
24 A. Nicolas and S. A. Safran, *Biophys. J.*, 2006, **91**, 61–73.
25 Y. Paran, I. Lavelin, S. Naffar-Abu-Amara, S. Winograd-Katz, Y. Liron, B. Geiger and Z. Kam, *Methods Enzymol.*, 2006, **414**, 228–47.
26 C. M. Laukaitis, D. J. Webb, K. Donais and A. F. Horwitz, *J. Cell Biol.*, 2001, **153**, 1427–1440.
27 E. Zamir, B. Z. Katz, S. Aota, K. M. Yamada, B. Geiger and Z. Kam, *J. Cell Sci.*, 1999, **112**, 1655–1669.
28 R. Zaidel-Bar, S. Itzkovitz, A. Ma'ayan, R. Iyengar and B. Geiger, *Nat. Cell Biol.*, 2007, **9**, 858–868.
29 C. Ballestrem, B. Hinz, B. A. Imhof and B. Wehrle-Haller, *J. Cell Biol.*, 2001, **155**, 1319–1332.
30 M. A. Digman, C. M. Brown, A. R. Horwitz, W. W. Mantulin and E. Gratton, *Biophys. J.*, 2008, **94**, 2819–2831.
31 We recently became aware of a paper (B. Sabass, G. L. Gardel, C. M. Waterman and U. S. Schwarz, *Biophys. J.*, 2008, **94**, 207–220, ) in which a convoluted technique is proposed to significantly improve both the resolution and reliability of local traction forces. Such work has the potential to provide much needed data for verification of the current and other theoretical stress profiles along FA sites.